




Carrier Assisted Differential Detection With Generalized and Simplified Receiver Structure

Honglin Ji , Shuangyu Dong, Zhaopeng Xu , Jingchi Li , Ranjith Rajasekharan Unnithan , *Member, IEEE*, Yikai Su , *Senior Member, IEEE*, and William Shieh , *Fellow, IEEE*

Abstract—Coherent detection has the primary advantage of optical field recovery, which enables channel impairment compensation and advanced modulation formats for high-capacity transmission. On the other hand, direct detection (DD) is more cost-effective due to its local oscillator (LO)-free detection. To gain the field recovery advantage while preserving the LO-free detection for DD-based receivers, carrier assisted differential detection (CADD) has been proposed to retrieve the complex-valued double-sideband (DSB) signal. In this paper, to extend the concept of CADD, we propose a simplified CADD scheme with reduced hardware complexity and present signal-to-signal beating interference (SSBI) iterative mitigation algorithms with and without symbol decision. The required number of photodetectors and analog-digital converters (ADCs) for the simplified CADD receiver becomes the same as the coherent homodyne counterpart but without needing the expensive narrow-linewidth LOs. The performance of the proposed simplified CADD receiver is evaluated by 60-Gbaud 16-QAM DSB signals. Extensive performance comparisons are made between (i) the generalized CADD receivers with and without the simplified receiver structure, (ii) SSBI iterative mitigation algorithm with and without the symbol decision, and (iii) single carrier (SC) and OFDM-modulated DSB signals for the simplified CADD receiver.

Index Terms—Carrier assisted differential detection, complex-valued double-sideband signal, direct detection, optical field recovery, self-coherent homodyne detection, short-reach optical communications.

I. INTRODUCTION

COHERENT detection has achieved resounding success in optical fiber communications for multi-terabit transmission since 2009 [1]–[4]. The primary advantage of coherent detection is that it can recover the optical field thus the imperfect channel response, such as chromatic dispersion, bandwidth-limited optoelectrical components, and fiber nonlinearity could

Manuscript received August 12, 2021; revised September 16, 2021; accepted September 17, 2021. Date of publication September 21, 2021; date of current version November 16, 2021. This work was supported by the Australian Research Council (ARC) under Discovery Grants DP150101864 and DP190103724. (Corresponding author: Honglin Ji.)

Honglin Ji, Shuangyu Dong, Zhaopeng Xu, Ranjith Rajasekharan Unnithan, and William Shieh are with the Department of Electrical and Electronic Engineering, The University of Melbourne, Melbourne, VIC 3010, Australia (e-mail: honglinj@student.unimelb.edu.au; shuangyud@student.unimelb.edu.au; zhaopeng@student.unimelb.edu.au; r.ranjith@unimelb.edu.au; shiehw@unimelb.edu.au).

Jingchi Li and Yikai Su are with the State Key Laboratory of Advanced Optical Communication Systems and Networks, Department of Electronic Engineering, Shanghai Jiao Tong University, Shanghai 200240, China (e-mail: Jingchi_Lee@sjtu.edu.cn; yikaisu@sjtu.edu.cn).

Color versions of one or more figures in this article are available at <https://doi.org/10.1109/JLT.2021.3114235>.

Digital Object Identifier 10.1109/JLT.2021.3114235

be compensated using powerful digital signal processing (DSP) algorithms. As a result, high-order or probabilistic constellation shaped (PCS) modulation formats could be enabled for coherent detection-based systems to approach the Shannon capacity [5], [6]. Hence, coherent detection is primarily deployed in long- and medium-reach applications, seemingly promising for short-reach applications. However, it is still considered to be of high cost for short-reach optical interconnects due to needing narrow-linewidth laser sources for the transmitter and receiver. Moreover, the sophisticated wavelength alignment between the transmitter and receiver in coherent detection is required to minimize the frequency offset, which also increases the operational cost of managing laser sources. Until now, the conventional DD, namely, intensity modulation and direct detection (IMDD), is preferred for short-reach applications since it possesses the unique advantage of a LO-free receiver, which outperforms the coherent detection in hardware and operational cost. Without a need for LOs for the receiver side, DD relaxes the tight requirements on the wavelength stability and laser linewidth compared with the coherent detection. In consequence, un-cooled laser sources, such as distributed feedback (DFB) lasers, could be employed for DD-based transmission systems. Moreover, since DD could achieve self-homodyne detection, the complexity of required DSP algorithms could also be simplified for the carrier/phase recovery stage. However, the conventional DD can perform intensity-only detection and lose the phase information. Without the optical field information, the fiber chromatic dispersion poses a great challenge on the conventional DD systems and induces the intrinsic frequency-selective power fading in the received signal spectrum. Thus, the conventional DD systems have scaling challenges for achieving high-capacity transmission and elongating the transmission reach as well.

Therefore, to combine the advantages of both coherent detection and DD, the advanced DD receiver with the capability of retrieving the optical field has become the interest of researchers in industry and academia. Many efforts have been put into achieving such an advanced DD receiver that bridges the gap between conventional DD and coherent detection. To be capable of dispersion compensation for the conventional DD systems, the single-ended heterodyne detection [7], [8] has been studied to recover the optical field of the intensity-modulated signal for dispersion compensation, and the transmission distance is greatly extended compared with the conventional DD. To address the problem of intensity-only detection in the conventional DD receiver, the single-sideband (SSB) based modulation and

detection schemes, such as offset-SSB [9], virtual SSB-OFDM [10], subcarrier-interleaved OFDM [11], and Kramers-Kronig coherent receiver [12], have been proposed to extract the phase information from the received intensity signals. Nonetheless, the modulation format for these receiver schemes is all restrained to be SSB signals, which conspicuously halves the electrical spectral efficiency (SE) due to the self-heterodyne detection and is rather undesirable. As the optical in-phase/quadrature (IQ) modulator can directly generate the DSB signal without sacrificing the available electrical bandwidth, it is indispensable for the advanced DD receivers to be capable of recovering the complex-valued DSB signal analogous to the coherent detection receiver. To recover the complex-valued DSB signal by DD receivers, block-wise phase (BPS) switching scheme [13] for either main-carrier or subcarriers of two consecutive signal blocks and signal-carrier interleaved DD scheme [14] in the time domain have been proposed for coherent-like detection without the intrinsic power fading in DD. However, either the electrical or optical SE of them is sacrificed and cannot achieve the level of coherent detection. Additionally, the phase retrieval technique originally developed in imaging has been applied for optical communication without needing a main optical carrier [15], [16]. Alternatively, from the second-order signal-signal beating term between the original and delayed signal, the complex-valued DSB can be recovered by the carrier-less differential detection receiver [17]. However, without the optical carrier for detection, the required electrical bandwidth is normally doubled to accommodate the second-order beating terms due to the square-law detection of the photodiodes.

Most recently, we put forward the CADD [18]–[21] scheme for retrieving the complex-valued DSB with a receiver structure equivalent to a delay interferometer. Beyond the originally proposed delay interferometer-based receiver structure, the concept of CADD is extended to use a generalized optical filter instead of the pure optical delay in the conventional CADD receiver [22].

In our previous work [23], we proposed the generalized CADD scheme with a simplified receiver structure to further reduce the hardware complexity, where the single-ended photodetector is avoided and part of the differential detection is achieved in the digital domain to obtain the linear signal-to-carrier beating term. The SSBI iterative mitigation algorithm with symbol decision was proposed for the simplified CADD receiver to cope with the SSBI and retrieve the complex-valued DSB signal. In this paper, we extend our previous work in detail and provide further discussions for our proposed generalized CADD with a simplified receiver structure in a comprehensive manner. As the symbol decision in the SSBI iterative mitigation algorithm could consume significant computation resources and power, we here propose the SSBI iterative mitigation algorithm without symbol decision for the simplified CADD receiver. The performance of the SSBI iterative mitigation algorithm without symbol decision is evaluated and compared with the symbol-decision-based one including the carrier-to-signal power ratio (CSPR) dependence, required iteration numbers, and optical signal-to-noise ratio (OSNR) performance. Moreover, for generating the complex-valued DSB signal, the two modulation formats: time-domain SC modulation and frequency-domain

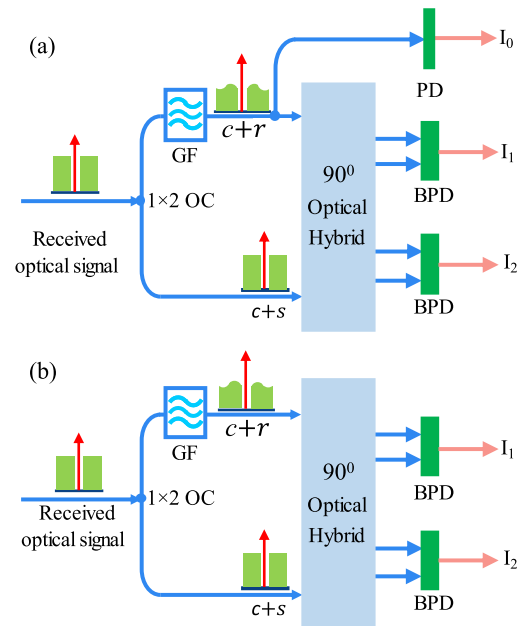


Fig. 1. Generalized CADD (a) without and (b) with a simplified receiver configuration. GF: generalized optical filter. PD: single-ended photodiode. BPD: balanced photodiode. OC: optical coupler.

OFDM modulation are prevailing in communication systems. Consequently, the performance comparison between SC and OFDM signals is also made in this paper for the generalized CADD with a simplified receiver structure. Finally, the wavelength drift tolerance of various receiver schemes, algorithms, and modulation formats are compared in this paper.

The paper is organized as follows: Section II presents the principle of the generalized CADD with/without the simplified receiver structure and the required SSBI iterative mitigation algorithm with/without symbol decision. Section III performs the numerical analysis for the proposed receiver structure and algorithms and makes comparisons for them. Section IV concludes the paper.

II. PRINCIPLE OF THE GENERALIZED CADD SCHEME AND SSBI ITERATIVE MITIGATION ALGORITHM

A. Generalized CADD Without Simplified Receiver Structure

The generalized CADD without a simplified receiver structure is shown in Fig. 1(a). The received DSB optical signal containing the self-coherent homodyne optical carrier is first equally split into two branches, one of which passes through the generalized optical filter (GF). The GF could be: (1) pure optical delay, which is the conventional CADD receiver; (2) phase-only filters, such as the chromatic dispersion; (3) optical filters having bandpass characteristics and arbitrary group delay [22]. Then the two branches are fed into the 90-degree optical hybrid for differential detection and the filtered branch is also detected by using a single-ended photodiode. For explanation simplicity, all physical efficiency of the used optoelectrical components in the CADD receiver is assumed to be unit on the received signals, such as optical couplers and the responsivity of the photodiodes.

Let c be the constant optical carrier and $s(t)$ be a complex-valued DSB signal without loss of generality, which could be generated by either time-domain SC or frequency-domain OFDM modulation. The received optical signal could be denoted as $c + s(t)$. We assume the generalized filter (GF) has no filtering effects on the constant optical carrier, namely, the amplitude of the carrier is maintained after passing through the GF since the constant optical carrier is commonly used to linearize the optical channel. After the GF, the generated optical signal is expressed as $c + r(t)$ where

$$r(t) = s(t) \otimes T(t) \quad (1)$$

(\otimes stands for convolution operation, $T(t)$ is the time-domain impulse response of the GF). Note that the GF could have a phase response coefficient on the constant optical carrier c , which could be factored out and lumped into the impulse response $T(t)$. From the three photodetectors, the output waveforms are given by

$$I_0 = |c + r|^2 = |c|^2 + |r|^2 + rc^* + r^*c \quad (2)$$

$$I_1 = \text{Re}[(c + s) \cdot (c + r)^*] \quad (3)$$

$$I_2 = \text{Im}[(c + s) \cdot (c + r)^*] \quad (4)$$

where ‘*’ stands for complex conjugate; $\text{Re}[\cdot]$ and $\text{Im}[\cdot]$ take the real and imaginary parts of a complex variable, respectively. Combining Eqs. (2-4) to eliminate the conjugate linear terms, a digitally reconstructed signal R_1 can be derived as

$$R_1 = I_1 + jI_2 - I_0 = (s - r) c^* + SSBI_1 \quad (5)$$

where $SSBI_1 = r^* (s - r)$ and the first term is desired for complex-valued DSB signal recovery. Compared with the conventional CADD receiver using pure optical delay, the power of the $SSBI_1$ could be greatly suppressed by using a narrow optical filter for the generalized CADD receiver, which benefits for the performance improvement. Therefore, a linear replica of the received DSB signal in the frequency domain could be retrieved by

$$S(f) = \frac{1}{c^*} \frac{F(R_1 - SSBI_1)}{1 - T(f)} \quad (6)$$

where $F(\cdot)$ represents the Fourier transform, $T(f)$ is the frequency response of the GF $T(t)$. Therefore, for the generalized CADD receiver, the generalized transfer function is $H_1(f) = 1 - T(f)$. When the GF uses pure optical delay τ , $H_1(f) = 1 - e^{-j2\pi f\tau}$, which is just the transfer function of the conventional CADD receiver [18]. With the recovered optical field by the generalized CADD receiver, the channel impairments including chromatic dispersion could be compensated for high-order modulation formats.

B. Generalized CADD With a Simplified Receiver Structure

Fig. 1(b) illustrates the generalized CADD with a simplified receiver structure. Compared with the generalized CADD receiver shown in Fig. 1(a), the single-ended photodetector is saved. As such, the front-end complexity of the generalized CADD receiver is further simplified. It can be observed that the required number of balanced photodetectors and ADCs is the

same as the coherent homodyne receiver but without needing the expensive narrow-linewidth LO. In addition, the simplified CADD receiver achieves self-coherent homodyne detection.

By only utilizing the two balanced photodetectors outputs I_1 and I_2 , the signal R_2 can be digitally recombined as

$$\begin{aligned} R_2 &= I_1 + jI_2 - [(I_1 + jI_2) \otimes T]^* \\ &= sc^* - rc^* \otimes T^* + sr^* - s^*r \otimes T^* \end{aligned} \quad (7)$$

In the simplified CADD receiver, the produced SSBI becomes $SSBI_2 = sr^* - s^*r \otimes T^*$. In Eq. (7), to digitally reconstruct the signal R_2 , the filter response $T(t)$ of the used GF needs to be known in advance. However, the equivalent filter response of an optical filter at the baseband is normally unknown. To estimate the filter response of the used GF, the training sequence for the simplified CADD receiver is required, which will be detailed in the next section. Similar to the generalized CADD receiver, the received complex-valued DSB signal in the frequency domain can be acquired by

$$S(f) = \frac{1}{c^*} \frac{F(R_2 - SSBI_2)}{1 - T(f)T^*(-f)} \quad (8)$$

Consequently, the generalized transfer function for the simplified CADD receiver is $H_2(f) = 1 - T(f)T^*(-f)$. Compared with the generalized CADD receiver, the equivalent GF of the simplified CADD receiver is $T(f)T^*(-f)$, which is a cascade of two GFs with a mutually conjugated time-domain impulse response. Therefore, the equivalent or cascaded GFs could have a sharper roll-off edge compared with the only one GF in the generalized CADD receiver. As a result, the second-order SSBI could be further restrained and the simplified CADD receiver will perform better than the generalized CADD receiver. Note that some GFs with even symmetry in phase response like chromatic dispersion could not be employed for the simplified CADD receiver as the frequency response of the chromatic dispersion has a quadratic relation with the frequency and the equivalent GF of the simplified CADD receiver is unit generating zero transfer function.

In the CADD receiver, its transfer function would have null or close-to-zero magnitude at the zero frequency as the center frequency of the GF is normally the same as the transmitted constant optical carrier. Moreover, the intrinsic SSBI of the CADD receiver has a approximately triangle shape in the frequency domain. At the zero frequency, the SSBI is the most severe. After applying the inverse of the transfer function to retrieve the received DSB signal, the signal components including SSBI and noise at the low-frequency region could be amplified when the magnitude of the generalized transfer function is smaller than 1. Thus, the signal quality at the low-frequency region could deteriorate. To avoid such performance degradation, a frequency guard band between the upper and lower sideband is adopted. A large frequency guard for the CADD receiver benefits the performance improvement while sacrificing the electrical SE. Therefore, there is a trade-off between the electrical SE and transmission performance. It is noted that the frequency guard band is generally small and not intended to accommodate all SSBI.

C. SSBI Iterative Mitigation Algorithm

Due to the DD-based receiver structure in nature, various CADD schemes suffer from severe SSBI. To combat the SSBI, high CSPR is preferred to enhance linear signal-carrier beating terms and suppress the SSBI. However, high CSPR could lower the OSNR sensitivity as the constant optical carrier occupies a large portion of the total signal power. To manage the SSBI by DSP, SSBI iterative mitigation algorithm that has been widely employed for SSB-based receivers [10], [24] could be also adopted for CADD receivers. The SSBI iterative mitigation algorithm for the generalized CADD without simplified receiver structure has been presented in [22]. We here only discuss the SSBI iterative mitigation algorithm for the simplified CADD.

For the simplified CADD receiver, the filter response $T(t)/T(f)$ of the GF is required to be estimated for digitally reconstructing the signal R_2 after obtaining the signal $I_1 + jI_2$. Since the received signal $I_1 + jI_2$ contains linear, conjugate linear, and SSBI terms, the probe signal can be formatted in OFDM-based SSB signal with interleaved subcarriers, where only the odd subcarriers are filled with symbols to avoid the contamination of SSBI and the rest subcarriers are empty. To estimate the whole filter response in the spectrum of modulated DSB signal, the OFDM-based SSB signal on the lower and upper sideband could be separately sent. Taking advantage of the massive subcarriers structure of OFDM-modulated signal and the continuous filter response of the used GF, the interpolation in the frequency domain could be used to get the entire filter response $T(f)$ of the used GF in the spectrum of interest. Then the obtained filter response $T(f)$ could be applied to digitally reconstruct the required signal R_2 for complex-valued DSB signal recovery. The generalized transfer function $H_2(f)$ could be calculated by its expression using $T(f)$ or estimated by using the OFDM-based SSB training sequence again in the reconstructed signal R_2 .

The crux of the CADD receiver is to handle the intrinsic SSBI. Fig. 2 illustrates the SSBI iterative mitigation algorithms for the simplified CADD receiver with and without symbol decision. In the symbol-decision-based iterative algorithm as shown in Fig. 2(a), the accumulated chromatic dispersion (CD) and transfer function should be compensated before symbol decision and the CD should be again emulated after the symbol decision. In the SSBI iterative mitigation algorithm without symbol decision as shown in Fig. 2(b), the CD compensation and emulation are removed. Only the equalization of transfer function and direct current (DC) blocking are needed since the DC component could work as the constant carrier producing linear beating terms during the reconstruction of SSBI. As illustrated in Fig. 2, the first iteration of the SSBI iterative mitigation algorithm is preceded in the presence of the undesired SSBI. In the subsequent iterations, the SSBI reconstructed in the last iteration is subtracted from the digitally combined signal R_2 to improve the accuracy of SSBI reconstruction. Therefore, the essence of the iterative algorithm is to reconstruct the SSBI iteratively and accurately for the SSBI subtraction in DSP. The advantage of the symbol decision-based SSBI iterative mitigation algorithm is that the recovered signal $s(t)$ after symbol decision has no contamination from residual SSBI while the signal-to-noise beating interference (SNBI) and

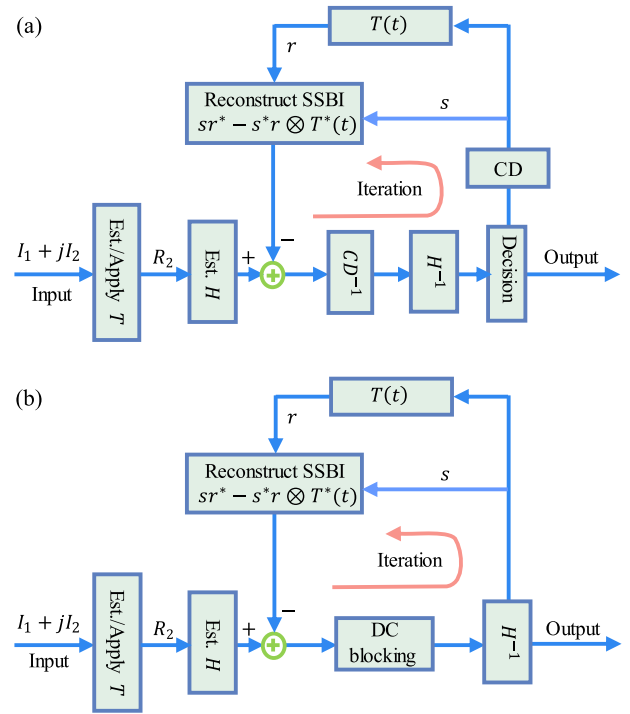


Fig. 2. SSBI iterative mitigation algorithm (a) with and (b) without symbol decision for simplified CADD receiver. Est. estimated. SSBI: signal-to-signal beating interference. CD: chromatic dispersion. DC: direct current component. H: transfer function. T: filter response of the GF used.

noise-to-noise beating interference (NNBI) cannot be eliminated, especially in a low-OSNR channel. The SSBI iterative mitigation algorithm without symbol decision has the advantage of low DSP complexity compared with the symbol decision based one. In addition, the signal and noise are regarded as a whole, which could eliminate the SNBI and NNBI. However, the disadvantage of the iterative algorithm without symbol decision is that residual SSBI cannot be avoided for reconstructing the SSBI, which will result in high-order SSBI during the iteration.

III. RESULTS AND DISCUSSIONS

A. Simulation Setup

To investigate the performance of the proposed generalized CADD receiver and the SSBI iterative mitigation algorithm, the simulation is carried out for both receivers with and without simplified receiver configuration. A 60-Gbaud 16-QAM signal with either OFDM or SC modulation format is employed for both receivers for a fair comparison, achieving a 240-Gb/s raw data rate. For the DSB signal based on OFDM modulation, the sampling rate is set as 80-GSa/s and the discrete Fourier transform (DFT) size is 4096, in which 3072 subcarriers are loaded with 16-QAM symbols. As the signals at the low-frequency region suffer from severe amplified SSBI, the middle subcarriers with 5-GHz width are reserved as the frequency guard band, representing only 8.3% of the spectrum redundancy. For the SC-modulated signal, the upper and lower sideband are separately generated with a 30G baud rate. The used roll-off factor for the pulse shaping

is 0.01. Therefore, the total baud rate for the SC-modulated signal is 60-Gbaud, which is the same as the OFDM-modulated signal. To realize the same 5-GHz frequency guard band for the SC-modulated DSB signal, the upper and lower sideband are up-converted to two symmetric intermediate frequencies with ± 17.5 -GHz frequency, respectively. The generation of the DSB signal based on SC modulation is just like the twin-SSB signal [25]. To estimate the filter response and transfer function of the CADD receiver, the subcarrier-interleaved OFDM probe signal with SSB modulation format is employed and added at the beginning of the payload. The frequency response of the used filters or transfer functions is averaged over 20 samples at each frequency point. The constant optical carrier without linewidth effect is added to the DSB signal at the transmitter before fiber transmission according to the needed CSPP values. The signal power in calculation includes the constant optical carrier, probe signal, and information-bearing DSB signal. The transmission distance is 1000 km with 17-ps/nm/km dispersion coefficient. Note that the 1000-km transmission reach is only used to evaluate the dispersion tolerance of CADD receivers. In short-reach optical communications, the transmission distance is normally tens of kilometers. After the fiber transmission, the received DSB signal propagating with the constant optical carrier is added with the additive white Gaussian noise (AWGN) according to the designated OSNR. The theoretical OSNR is calculated by $OSNR = \frac{\rho E_s}{2N_o B_{ref}}$, where E_s is the signal power including the information-bearing signals and constant optical carrier; N_o is the power spectrum density of the AWGN noise; B_{ref} is the 0.1-nm reference spectrum bandwidth; signal power scaling factor $\rho = 1$ for single-polarization signal and $\rho = 2$ for dual-polarization signal. In paper [22], [23], to be consistent with the dual-polarization transmission systems, the power scaling factor ρ for the OSNR definition is set to be 2. In this paper, we adopt $\rho = 1$ for the OSNR definition as our transmitted signal is single-polarization in practice. On the receiver side, to focus on the impact of optical noise, the photodiodes are modeled as an ideal without dark current, shot noise, and thermal noise.

As one realization of the GF for the generalized CADD receivers, micro ring resonator (MRR) [26] based optical filter with arbitrary group delay is utilized for the generalized CADD receivers rather than the pure optical delay in the conventional CADD receiver. The reason for using MRR-based filters is that they can be readily implemented and integrated on the silicon photonics platform. This will facilitate the silicon integration of our proposed DD-based CADD receivers.

Although the length accuracy of the optical path during the design of silicon photonics circuit can be readily managed within 1 micron, 27-ps optical delay is still chosen to be cascaded after the MRR-based optical filters to emulate the arbitrary group delay of the used GF. Another reason is that a large optical delay could sharpen the transfer function response at the low-frequency region and reduce the requirements on the frequency guard band. Fig. 3(a) shows the characteristics of the MRR-based optical filters with different 3-dB optical bandwidths. Note that we assume the system is optical noise dominated and there is an

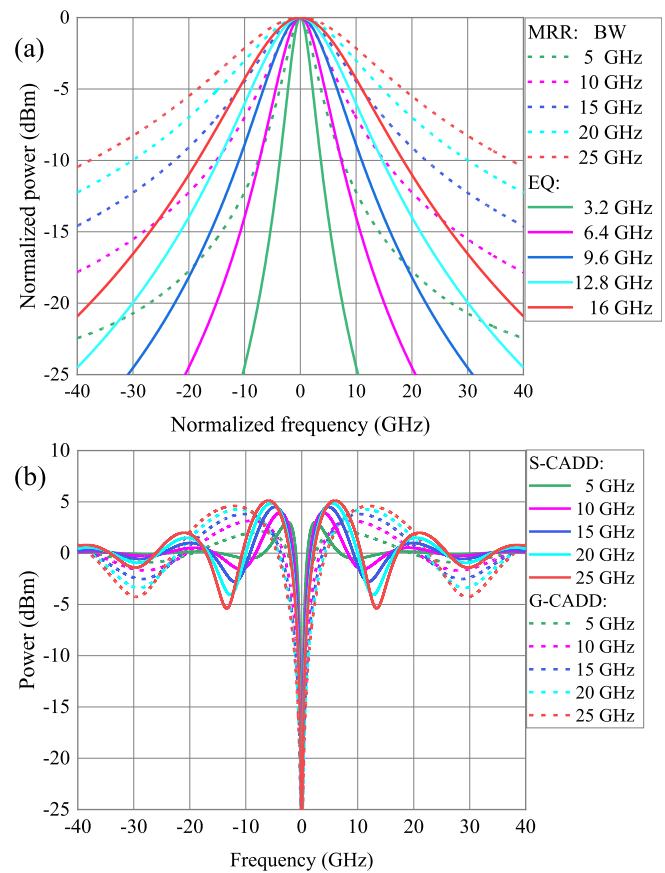


Fig. 3. (a) MRR based optical filter characteristic with different 3-dB bandwidths and the equivalent filter response for the simplified CADD receiver. (b) Transfer functions of the generalized and simplified CADD receivers with different MRR-based optical filters. EQ: equivalent optical filter response for the simplified CADD. BW: 3-dB optical bandwidth. S/G-CADD: simplified/generalized CADD.

optical amplifier and on-chip polarization controller before the MRR circuit to compensate for its loss and align the state of polarization of input optical signals with the MRR-based optical filters, respectively. In Fig. 3(a), the frequency values of the optical filters are offset by subtracting the center wavelength of 1550 nm. With small 3-dB optical bandwidth, the MRR-based optical filter has a fast edge roll-off and the produced SSBI could be substantially suppressed. The equivalent optical filter with frequency response $T(f)T^*(-f)$ for the simplified CADD receiver is also depicted in Fig. 3(a). The corresponding 3-dB optical bandwidth is presented in the legend. Due to the concatenation of two conjugate optical filters, the 3-dB optical bandwidth of the equivalent optical filter is greatly decreased by 36%, which could further improve the performance of generalized CADD receivers. In other words, the 3-dB optical bandwidth of the equivalent optical filters is the same as the 6-dB optical bandwidth of the MRR-based optical filters, which significantly lowers the requirements on the silicon photonics design of the MRR-based optical filters. The theoretical transfer functions of the generalized and simplified CADD receivers are shown in Fig. 3(b). It can be seen that the transfer function of the simplified

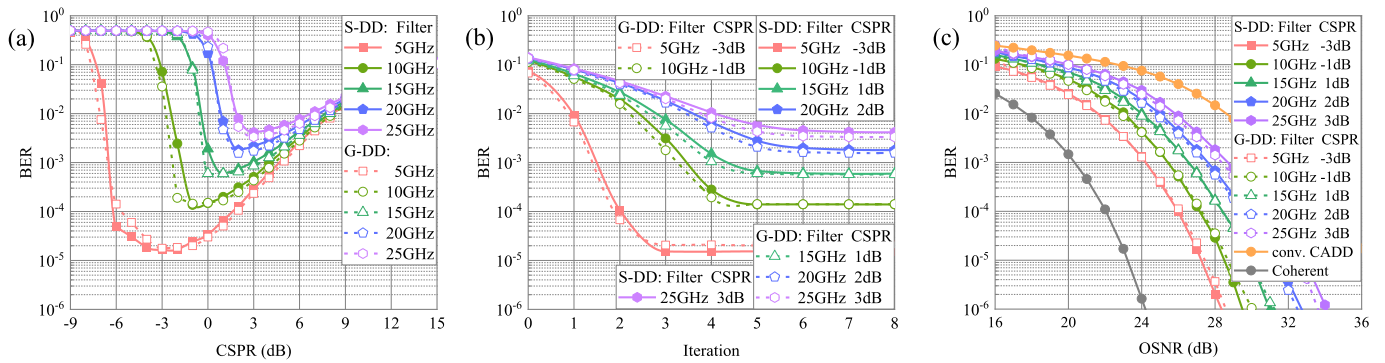


Fig. 4. Performance comparison between generalized and simplified CADD receiver. (a) BER versus CSRP for 60-Gbaud OFDM signal at 27-dB OSNR and after 1000-km transmission. (b) BER versus the iteration numbers at the optimal CSRPs and 27-dB OSNR, and 1000-km reach. (c) OSNR sensitivity comparison between the generalized and simplified CADD after 1000-km transmission. Conv. CADD: conventional CADD with pure optical delay. S/G-DD: simplified/generalized CADD receiver. BER: bit error rate.

CADD receiver has more fluctuations compared with the transfer functions of the generalized CADD receivers because the arbitrary group delay is equivalently doubled in the equivalent optical filter $T(f)T^*(-f)$ for the simplified CADD receiver. Thus, the second null point induced by the equivalently doubled optical delay moves into the signal spectrum but is partially avoided by the optical filter as shown in Fig. 3(b). Note that we utilize the subcarrier-interleaved OFDM-based SSB to estimate the filter response and transfer functions in the simulation though we have already known their theoretical response.

B. Performance Comparison Between Generalized and Simplified CADD Receivers

We first compare the performance of the generalized and simplified CADD receiver using the symbol decision-based SSBI iterative mitigation algorithm. The transmitted signal is a 60-Gbaud OFDM-formatted 16-QAM signal along with the training sequence for channel estimation. The performance comparison results are presented in Fig. 4. As the CSRP parameter is crucial for the SSBI iterative mitigation algorithm, the CSRP is first swept and optimized for both generalized and simplified CADD receiver after 1000-km transmission, which is shown in Fig. 4(a). Although high CSRP is preferred for optical channel linearizing, it sacrifices the information-bearing signal power under the same OSNR. Therefore, the optimal CSRPs for both of them with the five types of filters are the same and are -3 dB, -1 dB, 1 dB, 2 dB, and 3 dB, respectively. However, the required CSRP for Kramers-Kronig receiver is normally beyond 6 dB to meet the minimum phase condition and the CD could further increase the CSRP requirements due to the enhanced peak-to-average-power ratio (PAPR) after fiber transmission [27]. For the CADD receiver, the DSP complexity is directly related to the iteration numbers for the SSBI mitigation algorithm. With the optimal CSRPs for both CADD receivers, the required iteration numbers for the SSBI iterative cancellation algorithm are swept using the bit error rate (BER) as the metric of performance, which is presented in Fig. 4(b). The SSBI iterative mitigation algorithm requires the same iteration numbers for both CADD receivers to converge the BER performance and the needed iteration numbers are 3,

5, 5, 6, 6 for using the five MRR-based optical filters, respectively. With a large-bandwidth optical filter, the required iteration numbers are also large since the produced SSBI is strong and the iterative algorithm needs more iterations to improve the accuracy of the symbol decision. It can be also observed from Fig. 4(a)-(b) that the generalized CADD receiver without the simplified receiver structure only has slightly better BER performance. It could be attributed to the dispersion-aggravated distortion and the noise contaminated transfer function. Although the equivalent optical filter for the simplified CADD has smaller optical bandwidth, the performance improvement becomes marginal after AWGN channel and fiber transmission. The optimized iteration numbers are then used for subsequent OSNR sensitivity measurements. Fig. 4(c) illustrates the OSNR performance comparison between the conventional, generalized, simplified CADD and coherent detection after transmission. It is expected that the generalized and simplified CADD receivers show a similar BER performance. For convenience, the 1×10^{-2} BER level is taken as the hard decision-based FEC threshold here and also in subsequent sections unless otherwise stated. Compared with the conventional CADD receiver having the same data rate and guard band, the OSNR sensitivity of both generalized and simplified CADD receivers is improved by 7 dB using a 5 -GHz optical filter and 3 dB using a 25 -GHz optical filter. The OSNR sensitivity gap between the coherent detection and simplified CADD receiver using a 5 -GHz optical filter is shrunk to 3 dB. It indicates the advantage of using the narrow-bandwidth optical filters as the realizations of GF for CADD receivers.

C. Performance Comparison Between SSBI Iterative Mitigation Algorithm With and Without Symbol Decision

As discussed above, the generalized and simplified CADD receivers using symbol decision-based iterative algorithm have a similar performance including the CSRP dependence, required iteration numbers, and OSNR performance. In this section, we will investigate the performance of using the SSBI iterative mitigation algorithm with and without symbol decision for the simplified CADD receiver. The used modulation format is still the OFDM-modulated signal. The performance comparison

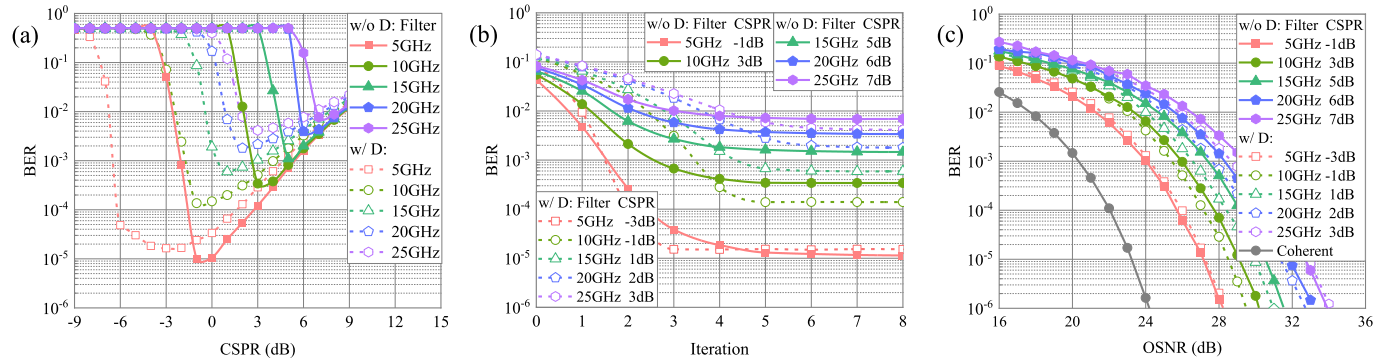


Fig. 5. Performance comparison between SSBI iterative mitigation algorithm with and without symbol decision for the simplified CADD receiver. (a) BER versus CSRP at 27-dB OSNR and after fiber transmission. (b) BER versus the iteration numbers at the optimal CSPRs and 27-dB OSNR, and 1000-km reach. (c) OSNR sensitivity comparison after transmission. w/(w/o) D: with/without symbol decision.

results are presented in Fig. 5. From Fig. 5(a), the CSRP dependence of using the iterative algorithm without symbol decision is consolidated. Higher CSRP is required for the simplified CADD receiver using the iterative algorithm without symbol decision, which could arise from the high-order SSBI during the iteration. The optimal CSPRs for the simplified CADD using the five different optical filters without symbol decision are -1 dB, 3 dB, 5 dB, 6 dB, and 7 dB, respectively. Operated at the optimal CSRP points, the required iteration numbers are shown in Fig. 5(b). By using the iterative algorithm without symbol decision, they all require 6 iterations to reach the stable BER performance, which is larger than the one with symbol decision. It manifests that the iterative algorithm with symbol decision has the advantage of no high-order SSBI and less iteration numbers. It can also be observed in Fig. 5(b) that the simplified CADD receiver using a large-bandwidth optical filter without symbol decision for iterative algorithm has a slightly worse BER performance due to the strong CSRP dependence. However, for using the 5-GHz optical filter, the simplified CADD without symbol decision has slightly better BER performance even with slightly higher CSRP, which could be attributed to the gradually getting smaller high-order SSBI during the iteration. The OSNR sensitivity comparison for the SSBI iterative cancellation algorithm is shown in Fig. 5(c). The OSNR sensitivity difference between the two algorithms is small and within 1 dB. However, the optimal CSRP for the two algorithms has a large discrepancy, which implies the OSNR sensitivity should also have a large difference. In theory, the OSNR sensitivity ratio between them can be calculated as

$$OSNR_{diff} = \frac{OSNR_{w}}{OSNR_{wo}} = \frac{CSPR_w + 1}{CSPR_{wo} + 1} \quad (9)$$

where $OSNR_w/OSNR_{wo}$ is the OSNR sensitivity with/without symbol decision; $CSPR_w/CSPR_{wo}$ is the used CSRP for the simplified CADD receiver using the iterative algorithm with/without symbol decision. Note that we here assume that after the SSBI iterative algorithm, the recovered DSB only suffers from the noise and the residual SSBI/SNBI/NNBI are not taken into consideration for Eq. (9). Therefore, according to the optimal CSPRs for the two algorithms, the theoretical OSNR sensitivity differences for using the five MRR-based optical filters should be 0.8 dB, 2.2 dB, 2.7 dB, 2.8 dB, and 3.0 dB, respectively. The theoretical

difference values are all larger than the obtained difference values in Fig. 5(c). It could be attributed to that the iterative algorithm with symbol decision removes the noise and residual SSBI during the SSBI reconstruction while the SNBI and NNBI cannot be eliminated. The iterative algorithm without symbol decision suffers from residual SSBI and noise during the SSBI reconstruction and generates high-order SSBI while the SNBI and NNBI could be mitigated, especially in the low-OSNR region. Hence, they all contribute to the reduced OSNR differences in the simulation.

D. Performance Comparison Between SC and OFDM Signal

In the derivation of the generalized CADD receiver, the transmitted/received signal is assumed to be a complex-valued DSB signal without loss of generality. In communication systems, OFDM and SC signals are two typical and different modulation formats. OFDM delivers the information in the frequency domain while the SC signal conveys messages in the time domain. This motivates us to investigate whether there is a performance difference between SC and OFDM-modulated signals in the CADD receiver. Therefore, we use the simplified CADD receiver without symbol decision to recover the SC- and OFDM-modulated signals and make comparisons between them. The comparison results between the two modulation formats are shown in Fig. 6. The CSRP dependence of the two modulation formats has a similar trend and the same optical CSRP values for using different optical filters for the simplified CADD receiver. It reveals that the CSRP is a modulation format-agnostic parameter. The BER performance as a function of iteration numbers is presented in Fig. 6(b), which emerges a large difference for the two modulation formats. The required iteration numbers for the SC signal using the five optical filters are $7, 7, 6, 6, 6$, respectively. The SC-modulated signal requires more iteration numbers than the OFDM-modulated signals. However, after the BER performance converges, the BER performance of the SC signal is all better than the OFDM signal. This could be explained by the following reasons. Due to the high-pass characteristic of the transfer function as shown in Fig. 3(b), the strong SSBI concentrates in the low-frequency region, and the signal at the low-frequency region is restricted. Therefore, the performance of the OFDM-modulated signal is partially

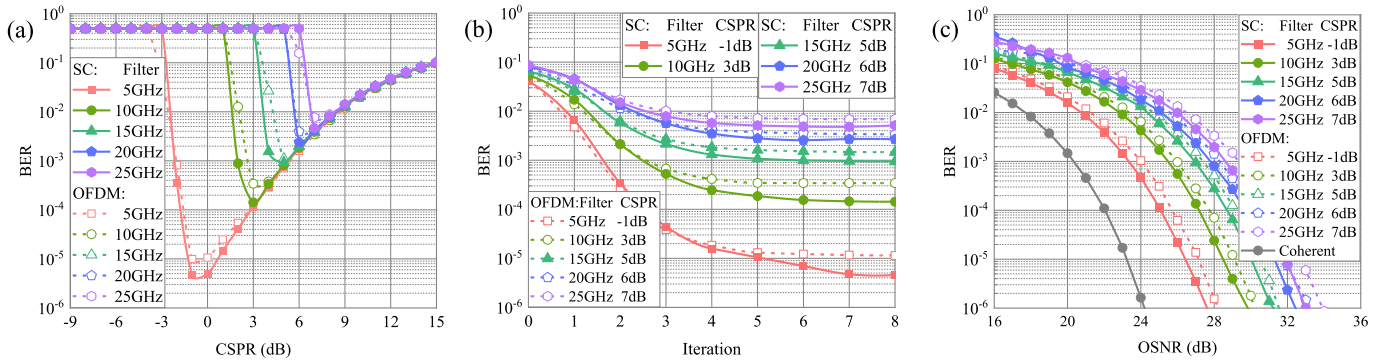


Fig. 6. Performance comparison between OFDM and SC modulated signal for the simplified CADD receiver using SSBI iterative mitigation algorithm without symbol decision. (a) BER versus CSRR at 27-dB OSNR and after fiber transmission. (b) BER versus the iteration numbers at the optimal CSRRs and 27-dB OSNR, and 1000-km reach. (c) OSNR sensitivity comparison after transmission.

limited by the low-frequency subcarriers while the performance of SC-signal is treated as a whole of the entire signal spectrum. It not only implies that the SC-modulated signal has better BER performance than the OFDM signal but also results in more iterations for the SC-modulated signal. Moreover, the OFDM-modulated signal achieves symbol decision in the frequency domain while the SSBI is generated in the time domain. It indicates that there is a low correlation between the SSBI and symbol decision for the OFDM-modulated signal. Consequently, the OFDM-modulated signal needs less iteration numbers than the SC-modulated signal. For the same reasons, another interesting phenomenon is observed that the SC-modulated signal using a smaller-bandwidth optical filter requires more iterations to get better performance instead while the OFDM-modulated signal has an inverse trend. Since the both SC- and OFDM-modulated signal has the same optimal CSRRs, they have the similar OSNR performance. It is also anticipated that the SC-modulated signal has a slightly better OSNR performance.

E. Wavelength Drift Tolerance of the Simplified CADD Receiver

The laser sources and silicon material-based MRR are sensitive to the temperature due to the change of effective refractive index of the material. For un-cooled lasers, such as DFB, they can have 9-nm wavelength lasing variation over a wide temperature range, typically -5°C to 85°C while it is within 1-GHz for external cavity lasers (ECLs). Thus, the wavelength drift tolerance for the simplified CADD receiver is needed to be investigated and the results are illustrated in Fig. 7. The wavelength drift tolerance for the generalized CADD has been studied in [22]. Due to the wavelength drift, the constant optical carrier could be attenuated and the filter response on the optical carrier should be taken into consideration during the derivation of the principle of simplified CADD receiver. The generalized transfer function for the simplified CADD receiver becomes $H_2(f) = \alpha^2 - T(f)T^*(-f)$ and the resulted SSBI is $SSBI_2 = \alpha sr^* - s^*r \otimes T^*$, where α is the response coefficient of the optical filter on the constant optical carrier. The response coefficient α can be estimated from the DC component of $I_1 + jI_2$ [22]. By changing the expressions of transfer functions and SSBI for the SSBI iterative mitigation algorithm as presented in Fig. 2, we simulate three

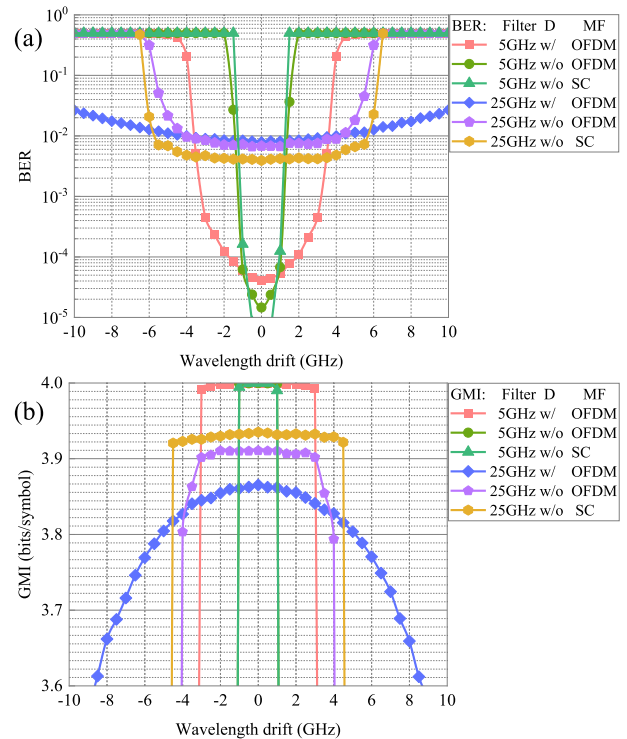


Fig. 7. (a) BER and (b) GMI performance of the simplified CADD versus the wavelength drift of the laser source at 27-dB OSNR after 1000-km transmission. D: symbol decision. w/(w/o): with/without symbol decision for SSBI iterative mitigation algorithm. MF: modulation format.

scenarios for the simplified CADD receiver: 1) with symbol decision-based SSBI iterative mitigation algorithm for OFDM signal; 2) SSBI iterative mitigation algorithm without symbol decision for OFDM-modulated signal; 3) SSBI iterative mitigation algorithm without symbol decision for SC-modulated signal. The used CSRRs are the corresponding optimal CSRRs for each scenario. The generalized mutual information (GMI) [5] is also measured since it can reliably quantify the maximum number of information bits per symbol with a vanishingly small error rate under the bit-metric decoding (BMD). It is anticipated that the BER and GMI performance deteriorates quickly due to the filtering effect-induced power reduction of the optical carrier. When the GMI penalty is 0.1 bits/symbol corresponding

to ~0.5-dB SNR penalty, the wavelength drift tolerance of the simplified CADD receiver using the 5-GHz optical filter for the three scenarios are 3 GHz, 1 GHz, and 1 GHz, respectively. For using the 25-GHz optical filter, they are 6 GHz, 4 GHz, and 4.5 GHz, respectively. With a large-bandwidth optical filter, it is reasonable that the CADD receiver is resilient against the wavelength drift. With the different modulation formats, the simplified CADD receiver has a similar wavelength drift tolerance. However, with symbol decision for the iterative algorithm, it has large tolerance of wavelength drift compared with the one without symbol decision since the symbol decision-based algorithm reconstructs the SSBI without the residual and high-order SSBI and noise, especially under the circumstance of the substantially weakened optical constant carrier. To increase the wavelength drift tolerance for CADD receivers, high CSPR at the expense of sacrificing the OSNR sensitivity is needed or the center of the MRR-based optical filters needs to be thermally adjusted.

IV. CONCLUSION

In this paper, we have proposed and investigated the generalized CADD with the simplified receiver structure and SSBI iterative mitigation algorithm with and without symbol decision. The proposed receiver requires the same number of balanced PDs and ADCs as the coherent homodyne counterpart but without needing the expensive coherent lasers. Compared with the generalized CADD receiver without a simplified receiver structure, the simplified CADD receiver can achieve a similar performance including the optimal CSPR, required iteration numbers, and OSNR sensitivity. For the SSBI iterative mitigation algorithm, symbol decision can reduce the algorithm dependence on the CSPR and iteration numbers but the OSNR performance has only a slight difference from the iterative algorithm without symbol decision. For the DSB complex signal, the SC-modulated signal for the simplified CADD receiver using SSBI iterative mitigation algorithm without symbol decision has a similar CSPR dependence and OSNR performance but requires more iterations. Finally, the wavelength drift tolerance between various algorithms and modulation formats are studied. The symbol decision-based SSBI iterative mitigation algorithm shows superiority and has a high tolerance of the wavelength drift. The wavelength drift tolerance for the simplified CADD receiver is modulation format-agnostic. In a nutshell, to have a low CSPR dependence, less iteration numbers and strong wavelength drift tolerance, the symbol decision-based SSBI mitigation algorithm is preferred. However, the OSNR sensitivity for the simplified CADD receivers with various iterative algorithms and modulation formats is similar. Therefore, the proposed simplified CADD scheme could be a good solution for low-cost and high-capacity applications.

REFERENCES

[1] Y. Ma, Q. Yang, Y. Tang, S. Chen, and W. Shieh, "1-Tb/s per Channel coherent optical OFDM transmission with subwavelength bandwidth access," in *Proc. Opt. Fiber Commun. Conf.*, 2009, Paper PDP1.

[2] S. Chandrasekhar, X. Liu, B. Zhu, and D. Peckham, "Transmission of a 1.2-Tb/s 24-carrier no-guard-interval coherent OFDM superchannel over 7200-km of ultra-large-area fiber," in *Proc. ECOC'09*, Vienna, Austria, 2009, Paper PD2.

[3] H. Masuda et al., "13.5-Tb/s (135 111-Gb/s/ch) no-guard-interval coherent OFDM transmission over 6248 km using SNR maximized second-order DRA in the extended L-band," in *Proc. OFC/NFOEC'09*, San Diego, CA, USA, 2009, Paper PDPB5.

[4] R. Dischler and F. Buchali, "Transmission of 1.2 Tb/s continuous wave-band PDM-OFDM-FDM signal with spectral efficiency of 3.3 bit/s/Hz over 400 km of SSMF," in *Proc. OFC/NFOEC'09*, San Diego, CA, USA, 2009, Paper PDP2.

[5] F. Buchali, G. Bocherer, W. Idler, L. Schmalen, P. Schulte, and F. Steiner, "Experimental demonstration of capacity increase and rate-adaptation by probabilistically shaped 64-QAM," in *Proc. Eur. Conf. Opt. Commun. (ECOC)*, Valencia, Spain, Sep. 2015, Paper PDP3.4.

[6] G. Böcherer, F. Steiner, and P. Schulte, "Bandwidth efficient and rate-matched low-density parity-check coded modulation," *IEEE Trans. Commun.*, vol. 63, no. 12, pp. 4651–4665, Dec. 2015.

[7] Q. Hu, R. Borkowski, K. Schuh, and H. Bülow, "Optical field reconstruction of real-valued modulation using a single-ended photoreceiver with half-symbol-rate bandwidth," *J. Lightw. Technol.*, vol. 39, no. 4, pp. 1194–1203, Feb. 2021.

[8] X. Li, M. Luo, C. Li, C. Yang, H. Li, and S. Yu, "Direct detection of pilot-assisted PAM-4 signals with large phase noise tolerance," *Opt. Lett.*, vol. 44, pp. 5457–5460, 2019.

[9] A. Lowery and J. Armstrong, "Orthogonal-frequency-division multiplexing for dispersion compensation of longhaul optical systems," *Opt. Exp.*, vol. 14, no. 6, pp. 2079–2084, 2006.

[10] W.-R. Peng et al., "Spectrally efficient direct-detected OFDM transmission employing an iterative estimation and cancellation technique," *Opt. Exp.*, vol. 17, no. 11, pp. 9099–9111, 2009.

[11] W.-R. Peng et al., "Theoretical and experimental investigations of direct-detected RF-tone assisted optical OFDM systems," *J. Lightw. Technol.*, vol. 27, no. 10, pp. 1332–1339, May 2009.

[12] A. Mecozzi, C. Antonelli, and M. Shtaiif, "Kramers–Kronig coherent receiver," *Optica*, vol. 3, no. 11, 2016, Art. no. 1220.

[13] X. Chen et al., "Block-wise phase switching for double-sideband direct detected optical OFDM signals," *Opt. Exp.*, vol. 21, no. 11, pp. 13436–13441, 2013.

[14] X. Chen, D. Che, A. Li, J. He, and W. Shieh, "Signal-carrier interleaved optical OFDM for direct detection optical communication," *Opt. Exp.*, vol. 21, no. 26, pp. 32501–32507, 2013.

[15] H. Chen, N. K. Fontaine, J. M. Gene, R. Ryf, D. T. Neilson, and G. Raybon, "Dual polarization full-field signal waveform reconstruction using intensity only measurements for coherent communications," *J. Lightw. Technol.*, vol. 38, no. 9, pp. 2587–2597, May 2020.

[16] Y. Yoshida, T. Umezawa, A. Kanno, and N. Yamamoto, "A phase-retrieving coherent receiver based on two-dimensional photodetector array," *J. Lightw. Technol.*, vol. 38, no. 1, pp. 90–100, Jan. 2020.

[17] X. Liu, S. Chandrasekhar, and A. Leven, "Digital self-coherent detection," *Opt. Exp.*, vol. 16, no. 2, pp. 792–803, 2008.

[18] W. Shieh, C. Sun, and H. Ji, "Carrier-assisted differential detection," *Light: Sci. Appl.*, vol. 9, no. 18, 2020.

[19] C. Sun, T. Ji, H. Ji, Z. Xu, and W. Shieh, "Experimental demonstration of Complex-valued DSB signal field recovery via direct detection," *IEEE Photon. Technol. Lett.*, vol. 32, no. 10, pp. 585–588, May 2020.

[20] T. Ji, C. Sun, H. Ji, Z. Xu, Y. Peng, and W. Shieh, "Theoretical and experimental investigations of interleaved carrier-assisted differential detection," *J. Lightw. Technol.*, vol. 39, no. 1, pp. 122–128, Jan. 2021.

[21] Y. Zhu, L. Li, Y. Fu, and W. Hu, "Symmetric carrier assisted differential detection receiver with low-complexity signal-signal beating interference mitigation," *Opt. Exp.*, vol. 28, no. 13, pp. 19008–19022, 2020.

[22] H. Ji, M. Sun, C. Sun, and W. Shieh, "Carrier assisted differential detection with a generalized transfer function," *Opt. Exp.*, vol. 28, no. 24, pp. 35946–35959, 2020.

[23] H. Ji, C. Sun, R. R. Unnithan, and W. Shieh, "Generalized carrier assisted differential detection with simplified receiver structure," in *Proc. Opt. Fiber Commun. Conf.*, 2021, Paper Th4D.2.

[24] Z. Li et al., "SSBI mitigation and the Kramers–Kronig scheme in single-sideband direct-detection transmission with receiver-based electronic dispersion compensation," *J. Lightw. Technol.*, vol. 35, no. 10, pp. 1887–1893, May 2017.

[25] S. Fan et al., "Twin-SSB direct detection transmission over 80km SSMF using kramers-kronig receiver," in *Proc. Eur. Conf. Opt. Commun.*, 2017, pp. 1–3.

[26] L. Chrostowski and M. Hochberg, *Silicon Photonics Design*. Cambridge, U. K.: Cambridge Univ., 2014.

[27] C. Sun, D. Che, H. Ji, and W. Shieh, "Study of chromatic dispersion impacts on Kramers–Kronig and SSBI iterative cancellation receiver," *IEEE Photon. Technol. Lett.*, vol. 31, no. 4, pp. 303–306, Feb. 2019.